

THE ANS COLLABORATION MONITORING PROGRAM

U. Munari¹ S. Bacci², L. Baldinelli², F. Castellani², G. Cetrulo², G. Cherini², S. Dallaporta², G. Dallavia², A. Englaro², A. Frigo², M. Graziani², V. Luppi², A. Maitan², C. Marangoni², A. Milani², S. Moretti², F. Moschini², P. Ochner¹, A. Siviero³, G. L. Righetti², S. Tomaselli², S. Tomasoni², A. Vagnozzi² and P. Valisa²

¹ *INAF Astronomical Observatory of Padova at Asiago, Italy*

² *ANS Collaboration, c/o Astronomical Observatory, Asiago, Italy*

³ *Department of Physics and Astronomy, University of Padova, Italy*

Received: 2011 December 2; accepted: 2011 December 15

Abstract. ANS Collaboration is a growing Italian network of small and medium size telescopes performing spectroscopy (low and medium resolution single dispersion, and Echelle high resolution modes) and $UBVR_CI_C$ CCD photometry of symbiotic stars and novae mainly, but with interest also on other types of objects like optical transients, eclipsing binaries, X-ray source counterparts and on-call follow-up observations of selected targets from some surveys like IPHAS or RAVE. In the present form ANS started operations in 2005, and at the time of writing has logged on symbiotic stars 14602 photometric runs and a rich ensemble of low and high resolution, absolutely fluxed spectra. The paper describes the internal organization, operation modes and procedures, and presents sample data and performance statistics.

Key words: stars: symbiotic binaries – stars: novae – photometry – spectroscopy

1. INTRODUCTION

ANS (*Asiago Novae and Symbiotic stars*) Collaboration¹ operates many different small/medium size telescopes located within Italy to the purpose of monitoring the photometric and spectroscopic evolution of all accessible novae and symbiotic stars. Other types of objects are also included in the observational program, like optical transients, eclipsing binaries or X-ray source counterparts. ANS is also engaged in providing on-call follow-up observations for selected targets of surveys like IPHAS or RAVE. In the present form, ANS started operations in 2005 and since then it is working smoothly. At earlier epochs, some of the observers and telescopes, now integral part of ANS, were already active in providing support to researches carried out with the professional telescopes of the Asiago observatory, which is jointly operated by the University of Padova (the 1.22 m telescope) and INAF National Institute of Astrophysics (the 1.82 m reflector, and the 67/92cm

¹<http://www.ans-collaboration.org>

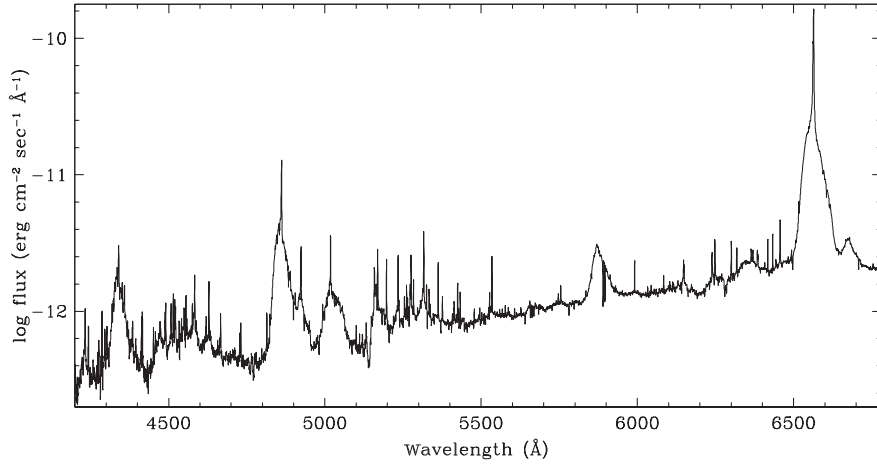


Fig. 1. A portion of an ANS Echelle high resolution spectrum of V407 Cyg for 2010 March 13 (UT 02:30), $t = +2.3$ days past optical maximum at $V = 8.67$, obtained by merging 19 adjacent Echelle orders (out of 31 recorded ones covering the 3950–8640 Å wavelength range) fluxed against red standards HR 7867 and HR 8228. The coexistence between the very sharp emission lines (Mira’s wind recombining after the ionization from the initial nova flash) and the broad lines (high velocity nova ejecta expanding through and colliding with the pre-existing Mira’s slow wind) is pretty obvious.

and 40/50cm Schmidt telescopes). All telescopes grouped by ANS are privately owned and supported, several of them being robotically or remotely operated.

2. SPECTROSCOPY

Two telescopes (60 cm and 70 cm reflectors) are currently devoted to spectroscopic observations both in the Echelle high resolution mode and the low/medium resolution single dispersion mode. The Cassegrain-fed spectrographs are self-designed and built to ensure the best compromise in terms of the weight, size, fast change of configuration, overall throughput and, in particular, accuracy of the performances (in terms of precision of radial velocities, suppression of scattered light, uniformity of resolving power, accuracy of absolute fluxing). The large format CCD detectors are of the thick, front-illuminated type to overcome the presence of fringing and thus to allow their use well into the far-red wavelength region. These thick detectors do not excel in sensitivity below 3900 Å but this is not a major concern, their use at the blue end of the optical range being compromised primarily by defocusing which affects commercial camera optics at such short wavelengths. To display some typical ANS results, Figure 1 illustrates the capability of accurate fluxing of Echelle spectra and merging their orders into 1D high resolution equivalents, Figure 2 shows an example of a routinely gathered low resolution, absolutely fluxed spectrum and Figure 3 zooms on a narrow region of an Echelle spectrum to highlight the resolving power potential.

Optical assemblies offering various fiber-fed comparison lamps are permanently mounted on the spectrographs to allow the possibility of on-the-fly selection of the type of comparison spectrum (Th, Ne-Ar, Fe-Ar) most suited for the selected

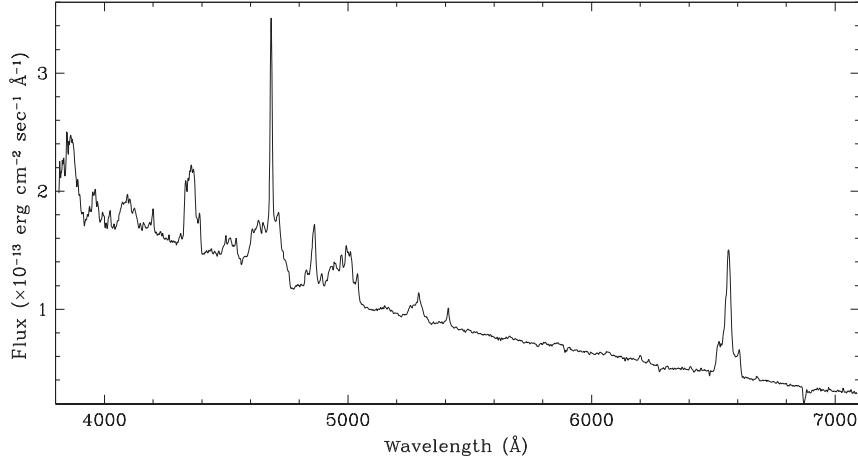


Fig. 2. ANS low resolution spectrum of Nova KT Eri 2009 on 2010 February 2, when the object was at $B = 11.46$, $V = 11.53$, $R_C = 11.37$, $I_C = 11.27$ and was declining from the outburst maximum peaking at $V = 5.4$ on 2009 November 14.7. The presence of a cool giant, the orbital period ~ 2 years (Jurđana-Šepić et al. 2012) and the high ionization emission lines of [Ne V] and [Ne III], probably present in quiescence (Nesci et al. 2009), make this recent nova likely a new symbiotic star.

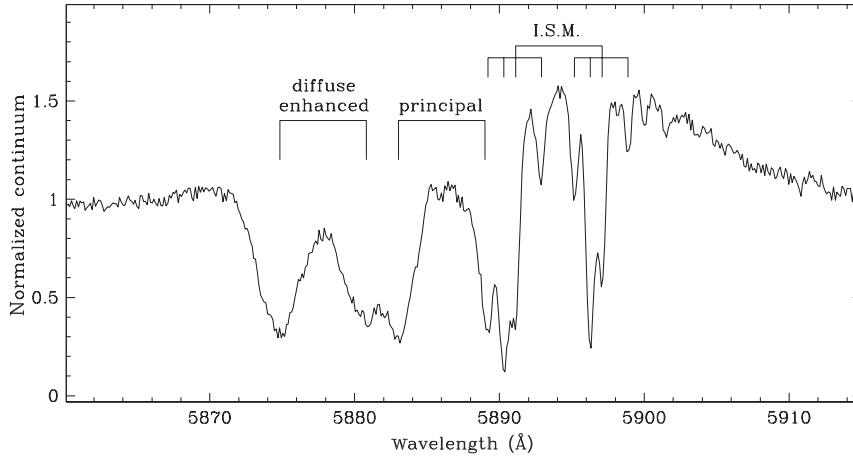


Fig. 3. The complex Na I D_{1,2} region for Nova Sct 2009 as recorded on an ANS Echelle high resolution spectrum on 2009 November 21, two days after the optical maximum and when the star was at $V = 7.6$. The resolving power is 17 000. At least four distinct interstellar components and both the *principal* and *diffuse enhanced* spectra of the nova are visible at the same time.

resolving power and wavelength range. Filters to cut the second-order spectra can be inserted in the optical path. The spectrographs rotate to the parallactic angle to compensate for wavelength dependent atmospheric refraction, so to ensure correct absolute fluxing over the entire wavelength range (especially important for novae,

which usually appear low on the southern horizon as seen from Italy). Manual or automatic guiding is performed on the TV image of the slit. The spectrographs currently in use represent the second generation of ANS instruments. The next generation in the making will include also the Stokes spectro-polarimetric modes (with a double Wollaston prism), the replacement of gratings by prisms for cross-dispersing in the Echelle spectrographs, and the introduction of wedges to separate the first and the second orders in low resolution spectra.

The majority of spectro-photometric standards available in the literature are too hot for proper use with such cool objects like the symbiotic stars or the (usually) heavily reddened novae. A blue leak from the grating second order is present in low-resolution optical spectra covering a wide wavelength range and causing an apparent flux deficiency at $\lambda \geq 7000 \text{ \AA}$ in the spectra of red objects fluxed with hot standards. To avoid the second exposure in the red through a blue-cutting filter, ASN has calibrated over the 3300–9900 \AA range a grid of 74 cool standards, located every hour in RA at the declination circles -15° , -3° and $+45^\circ$. The current calibration of these standards is characterized by contiguous steps 20 \AA wide, and the work is in progress to increase the resolution to 5 \AA steps for the application in the absolute fluxing of Echelle spectra. The photometric stability of these standards is proved by highly constant *Hipparcos* H_P measurements and by a routine ANS monitoring.

All the spectroscopic data reductions are carried out locally with IRAF, following standard recipes that each night involve the acquisition of suitable bias, dome flats, dark frames and observations of a consistent number of radial velocity, spectrophotometric and telluric standard stars. The finally reduced spectra and all the ancillary data (standard stars, derived calibration curves, applied flat and dark corrections, instrumental resolution pix-to-pix map, etc.) are then uploaded to the central ANS server and the logs updated.

3. PHOTOMETRY

The majority of telescopes operated by ANS are devoted to photometric monitoring. All of them observe in the B , V , R_C and I_C passbands, and those with ultraviolet transparent optics include also the U passband. SLOAN $u'g'r'i'z'$ filter sets are introduced in some instruments, and exploratory use of narrow-band filters (like $H\alpha$, [OIII], Strömngren b,y) is underway. A detailed look to ANS photometric filters, the local realizations of the Landolt's $UBVR_CI_C$ equatorial photometric system and the accuracy of the transformation to it are reviewed by Munari & Moretti (2012).

The ANS telescopes devoted to photometry range in size from 13 to 70 cm and are located from the sea level to mountain tops, and from rural to sub-urban areas. Target stars are assigned to them according to optimization criteria involving local sky background brightness, focal length, field of view, optical chain throughput, etc. The data are locally processed, under ANS central server supervision and continuous update of algorithms, with the proprietary ANS software. The continuously uploaded data are daily used to update light curves for all program stars.

Because all-sky photometric conditions does not apply to the majority of observing nights, and in a tight monitoring program non-photometric but clear nights cannot be wasted, the ANS operation mode is to adopt from external sources or self calibrate an accurate photometric comparison sequence around each program

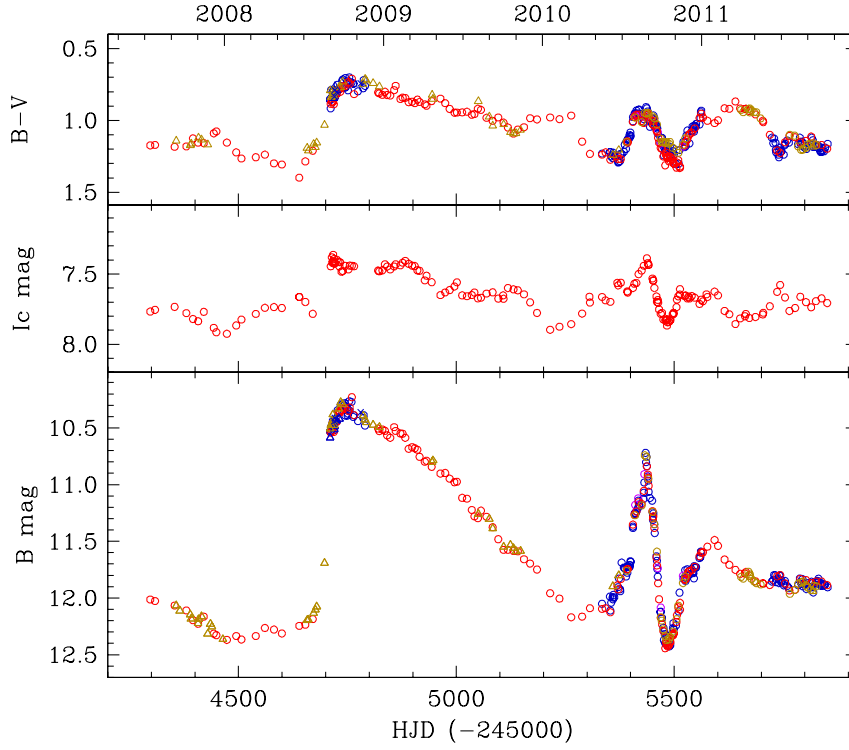


Fig. 4. The light curve of the current outburst of CI Cyg. Different symbols and colors identify data from different ANS telescopes.

star. This photometric sequence is then adopted for all telescopes observing that given target. This procedure effectively kills the random errors associated with the all-sky approach, leaving only the systematic part connected with the accuracy with which the photometric sequence has been calibrated and linked to the reference system (for ANS, the Landolt 1983, 1992 equatorial standards). Such a systematic offset, if any is actually present, will be exactly the same for all the telescopes observing the given star, and will not impinge on the quality and dispersion of the recorded light curves. For symbiotic stars, ANS adopts the $UBVR_C I_C$ photometric sequences calibrated around 81 objects by Henden & Munari (2000, 2001, 2006), who are currently working to extend the calibration of photometric sequences to the rest of known members of the class. For novae and other types of objects, calibrations are carried out on purpose, and usually made available via IBVS or included in the final published study of the given object.

ANS observations are scheduled to null or minimize the effect of seasonal conjunction of targets with the Sun. This of course frequently requires to catch a target very low at the horizon, just after sunset or shortly before dawn. Working in all-sky photometric calibration mode would made this type of observations unpractical and prone to large uncertainties. Calibrating against a local photometric sequence makes them similar to any other normal observation and keeps errors

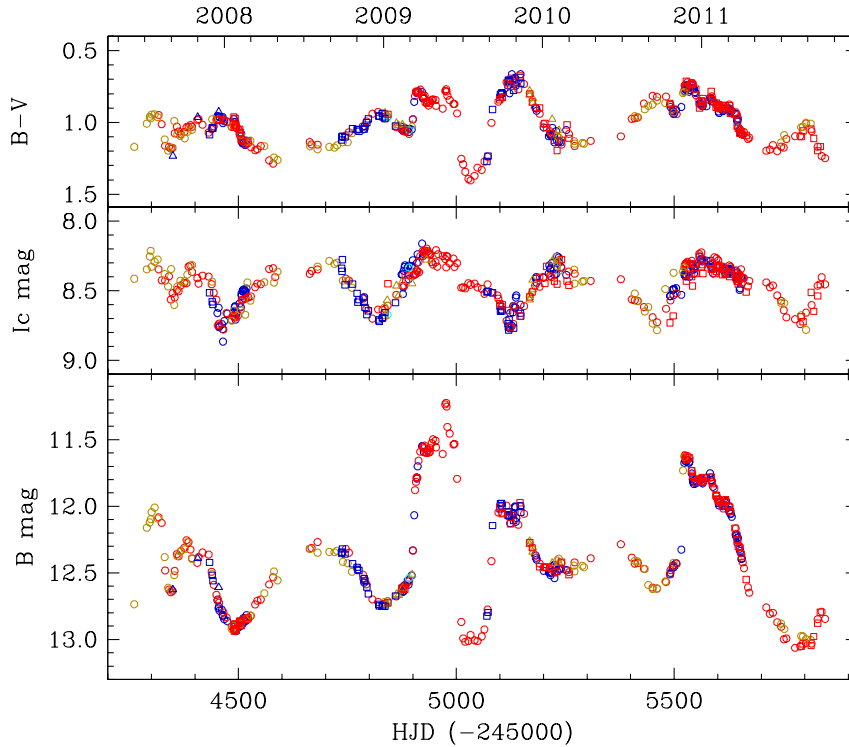


Fig. 5. The recent light curve of the classical symbiotic star AX Per. Different symbols and colors identify data from different ANS telescopes.

under strict control. Figures 4 and 5 present sample ANS light curves covering the last four years of two popular symbiotic stars, AX Per and CI Cyg. They illustrate a typical dispersion of ANS measurements and the absence of significant seasonal gaps.

Monitoring the program stars means also to continuously re-observe the corresponding photometric sequences, that can be checked for consistency and stability. This led to the discovery of a very few variable stars among the Henden & Munari sequences, which have been studied and published, and removed from the sequences in use (e.g., Munari et al. 2009, Siviero et al. 2010).

The ANS default mode to carry out the photometric measurement is via aperture photometry, while PSF-fitting is reserved to crowded fields or close pairs like QW Sge (this symbiotic star has an optical companion of similar brightness a few arcsec away), and PSF-fitting becomes the standard procedure with novae in the advanced decline, when they progressively return to obscurity in densely populated, low galactic latitude fields. The radius of the aperture is initially set to the FWHM of the PSF as averaged over all comparison stars, and is then automatically optimized (together with the internal and external radii of the sky annulus) to minimize the dispersion of the standard stars around the color-equations transforming the local system to the standard one. The slopes of the color-equations

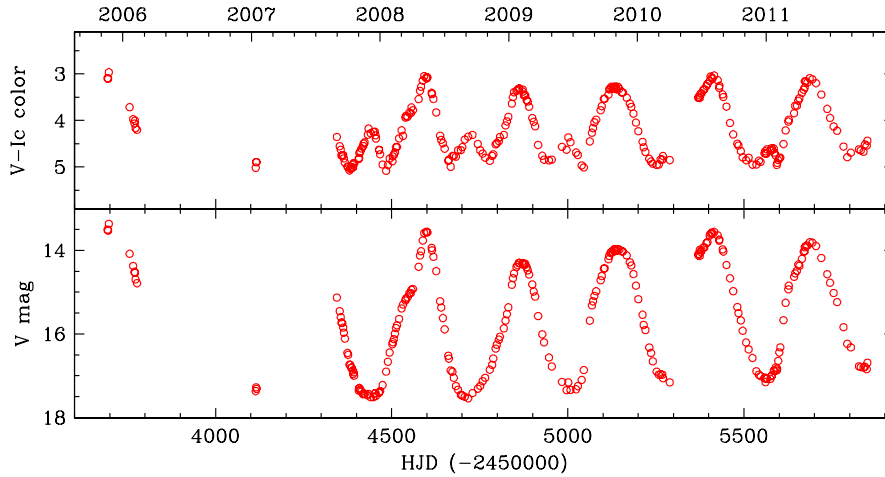


Fig. 6. The light curve of the dust-free symbiotic Mira LL Cas as monitored by the ANS telescope R030.

are then compared for consistency with those already in the database for the given instrument observing that target at similar airmasses and sky conditions. Deviations (quite unusual) are promptly signalled and the data extraction/reduction checked. To minimize seeing/guiding effects and disturbance from random events like cosmic ray hits, the total exposure time in a given filter is divided into multi-exposures, which are astrometrically registered and mean- or median-combined before being fed to the reduction pipeline.

At least two telescopes are usually assigned to a given target, so that their data can be mutually checked for instantaneous and long-term consistency. Examples of redundancy are evident in the light curves of AX Per and CI Cyg in Figures 4 and 5. Sometimes, an object is so faint and the required integration times so long that it is worth to assign only one instrument to its monitoring, as illustrated in Figure 6 for the dust-free symbiotic Mira LL Cas.

In addition to the target variable, photometry can be automatically performed for all stars present in the field. Each detected star is tagged astrometrically for object matching with previous observations of the same field and cross-identification with catalogs like USNO-B1 or 2MASS. The data on field stars are then automatically explored for transients or previously unknown variables, and incremental individual light curves are updated.

The output of the ANS photometric reduction pipeline provides a wealth of information to document the individual observations and monitor the quality of the data. The information is stored in about 70 columns trailing those reporting the value of the magnitude and color in the various bands. Among those of more direct use are: the total Poissonian error (including contributions from dark, sky and flat) on the variable and on the faintest and brightest of the comparison stars; the error of the sky flux for the variable and the median for the comparison stars; the number and range in color of the comparison stars, their rms around the color equation, its slope and associated error; the total error budget for the variable; location within the CCD dynamical range of the variable and the faintest and

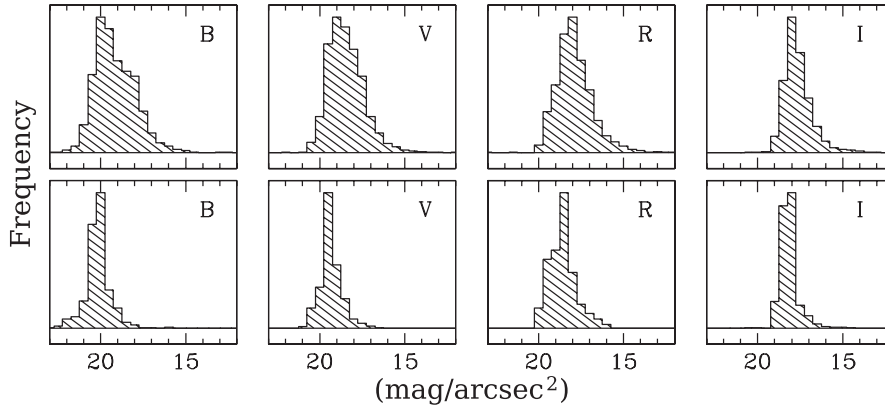


Fig. 7. The frequency distribution of the sky brightness (expressed as mag per arcsec²) in ANS observations of symbiotic stars. The upper row is the cumulative distribution of all observations, irrespective of the Moon phase and height above the horizon, sky conditions and zenith distance. The lower row still averages over all sky conditions but it is restricted to zenith distances $\leq 20^\circ$ and the Moon 10° below the local horizon.

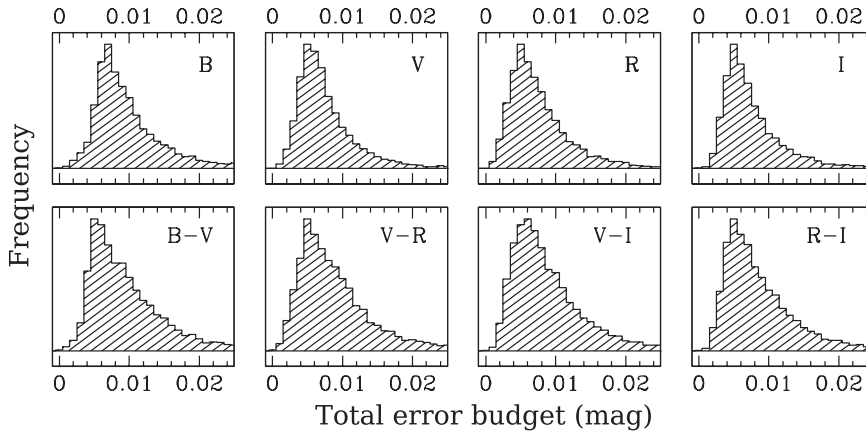


Fig. 8. Cumulative distribution, for passbands and colors, of the total error budget (expressed in magnitudes) for ANS observations of symbiotic stars.

brightest of comparison stars; ellipticity and tilt angle for the variable and the median for comparison stars; PSF radius, orientation and moments (2nd order, skewness and kurtosis) for comparison stars and the variable; proximity indicators for nearby field stars and their contamination threshold; the Moon phase, the height above the horizon and angular distance from the variable; the sky background brightness (mag/arcsec²), its uniformity and the airmass; the amount of vignetting in pre-flat-fielded images (as the ratio of the sky background flux in the four corners compared to center); all-sky conditions and transparency as recorded by automatic sensors or estimated by the operator (numerically coded).

Over the period from 2005 July 1 to 2011 July 1, ANS has logged 14602

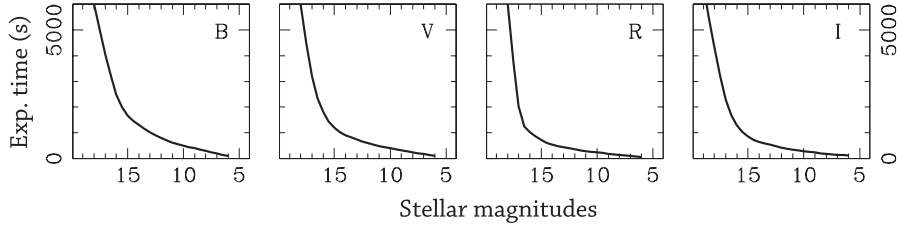


Fig. 9. Typical exposure times, in the various passbands, as a function of the target magnitude for a 30 cm aperture ANS telescope.

BVR_CI_C photometric runs of symbiotic stars. Only a small fraction of them included also the U passband, and for this reason the results in U have not been included in this paper. However, the number of ANS observations in this passband should increase in future. Figure 7 shows the distribution in sky background brightness of these 14602 observations. The sky background gets brighter with wavelength, a difference of ~ 2 mag between B and I_C is evident in Figure 7, in line with common experience. The comparison between top and bottom rows of Figure 7 illustrates well the effect of airmass and Moon phase on the recorded sky background. Figure 8 illustrates the distribution in the total error budget of all ANS observations of symbiotic binaries (note that the colors are obtained not as differences of magnitudes, but directly during the data reduction process). Finally, Figure 9 shows the dependence of the typical exposure times on target brightness for ANS observations with a 30 cm aperture telescope.

The ANS Collaboration data have so far made their way to tens of papers dealing mainly with in depth study of individual targets. For the future, a data release policy will be introduced, which will be based on data dumps by years, starting with 2012.

REFERENCES

- Jurdana-Šepić R., Ribeiro V. A. R. M., Darnley M. J., Munari U., Bode M. F. 2012, *A&A*, 537, A34
Henden A., Munari U. 2000, *A&AS*, 143, 343
Henden A., Munari U. 2001, *A&A*, 372, 145
Henden A., Munari U. 2006, *A&A*, 458, 339
Landolt A. U. 1983, *AJ*, 88, 439
Landolt A. U. 1992, *AJ*, 104, 340
Munari U., Siviero A., Dallaporta S. et al. 2009, *IBVS*, 5896
Munari U., Moretti S. 2012, *Baltic Astronomy*, 21, 22 (this issue)
Nesci R., Mickaelian A., Rossi C. 2009, *ATel*, 2338
Siviero A., Dallaporta S., Munari U. 2010, *IBVS*, 5936